Neutrino-induced muon flux deep underground and search for neutrino oscillations

T. K. Gaisser and Todor Stanev*
Bartol Research Foundation of The Franklin Institute, University of Delaware, Newark, Delaware 19716
(Received 23 January 1984)

We derive the flux of muons induced by interaction of ν_μ in rock as a function of neutrino energy and angle. Stopping muons come from relatively-low-energy neutrinos and therefore have somewhat greater potential sensitivity to neutrino oscillations than the higher-energy through-going muons, but their flux is lower.

I. INTRODUCTION

Cosmic rays incident on the atmosphere produce neutrinos, a small fraction of which interact in the Earth to produce a flux of horizontal and upward muons which are visible in underground detectors.[1-3] The flux of these muons is of the order of 3×10^{-13} cm^{-2}sec^{-1}sr^{-1} for $E>1$ GeV, much lower than the downward flux of surviving muons produced in the atmosphere, even for the deepest existing detectors. Downward-going neutrino-induced muons, though present, are therefore buried in the huge background of atmospheric muons. At very deep sites, ν-induced muons also exceed atmospheric background for angles somewhat above the horizontal ($\theta>55°$ at 8.9×10^5 g/cm^2 and $\theta>60°$ at 7.6×10^5 g/cm^2).[1,2]

Because the ν parents of upward muons travel distances up to the diameter of the Earth ($\sim1.3\times10^4$ km) after their production in the atmosphere, the flux of the muons induced by these neutrinos is in principle sensitive to flavor oscillations of neutrinos[4] in an unexplored range of neutrino mass parameters.[5] A necessary (but not sufficient) condition for observability of mixing is that the phase difference between relevant mass eigenstates be >1; i.e.,

$$[\Delta m^2\ (\mathrm{eV}^2)]>[E_\nu\ (\mathrm{GeV})]/[L\ (\mathrm{km})]$$
$$\sim[E_\nu\ (\mathrm{GeV})]\times10^{-4}\ \mathrm{eV}^2$$

for $L\sim10^4$ km.

The relative merits of neutrino interactions inside the detector as compared to ν-induced muons for the neutrino-oscillation search have been discussed by Ayres *et al.*[6] Despite the disadvantages of higher E_ν, unobservability of the downward flux of ν-induced muons, and rapid absorption (and hence unobservability) of the related ν_e-induced electrons, it is still worth considering ν-induced muons from this point of view for two reasons. First, they can be detected and measured more simply than contained interactions, and second (because of the higher E_ν involved) the divergence between the directions of the muon and the parent neutrino is on average smaller than the angle between ν and lepton in contained charged-current interactions.

To search for ν oscillations with ν-induced muons, however, one needs to know, for comparison, the absolute magnitude and angular dependence of the upward muon flux in the absence of oscillations. It is also essential to know the energy spectrum of the ν parents of the muons since the details of the oscillation phenomena expected in any particular mixing scheme (including effects of propagation in matter) will depend on a folding of the neutrino energy spectrum with the oscillation equations. In addition, both the magnitude of the neutrino-induced flux of muons and its characteristic angular dependence (which arises from the atmospheric-density effect at ν production) should be useful for detector calibration. Since earlier calculations of the flux of neutrino-induced muons[7,1-3] have not described all these details in a general way, and because they are of interest for a number of on-going underground experiments, we decided to repeat the calculations here. It turns out that the basic results can, to a good approximation, be expressed in a useful closed form.

II. MUON LUMINOSITY OF ROCK

The differential luminosity of the Earth in neutrino-induced muons is

$$\int S(E_\nu,E_\mu,\theta)dE_\nu=N_A\int\frac{d\sigma}{dE_\mu}\frac{dN}{dE_\nu}dE_\nu\ , \tag{1}$$

where N_A is Avogadro's number, $d\sigma/dE_\mu$ the charged-current cross section per nucleon for $\nu_\mu+N\rightarrow\mu+X$, and dN/dE_ν the differential neutrino flux at zenith angle θ. $\int S\,dE_\nu$ is in muons/(g sec sr GeV). The flux of muons through a detector element of area A is then obtained by integrating the muon luminosity over all distances R from the detector element, taking account of muon energy loss in the rock. We first discuss the computation of $S(E_\nu,E_\mu,\theta)$.

A. Neutrino spectrum

Typical large underground detectors will require muons of $E_\mu\geq1$ GeV at the detector for identification. Since both the muon range and the muon production cross section increase with energy, one needs the neutrino spectrum up to the TeV range to carry out the calculation. Recent calculations[8] of the neutrino flux in the 0.2—2-GeV range have emphasized angular and time dependence due to effects of the geomagnetic field and solar modulation, respectively. For the higher neutrino energies of interest here, these effects are relatively unimportant, and we therefore use the high-energy neutrino fluxes calculated by Volkova[9] for a range of zenith angles θ. The high-energy flux of nearly horizontal ν_μ is significantly larger (about a factor of 2 for $E_\nu \sim 10-100$ GeV) than the vertical flux because of the $\sec(\theta)$ enhancement of decay of the parent mesons that exists in an exponential atmosphere.

B. Charged-current cross sections

A sum over ν- and $\bar{\nu}$-induced muons is implied in Eq. (1). We therefore need separately the particle and antiparticle cross sections. The differential cross section in the parton model for deep-inelastic ν scattering on a target nucleon is[10]

$$\frac{d\sigma_\nu}{dx\,dy}=\frac{G^2 m E_\nu}{\pi}\frac{M_W{}^4}{(2mxyE_\nu+M_W{}^2)^2}\times\{q(x)+s(x)+[\bar{q}(x)-\bar{s}(x)](1-y)^2\}\ , \quad (2)$$

where $y=1-E_\mu/E_\nu$, $2mxyE_\nu=|Q^2|$, and m is the nucleon mass. Here

$$q(x)\equiv u(x)+d(x)+s(x)$$

is the quark structure function normalized so that, e.g.,

$$\int_0^1 u(x)\,dx\cong 0.29$$

is the fraction of the momentum of a proton carried by up quarks, etc. The corresponding expression for scattering of an antineutrino involves the interchange $q\leftrightarrow\bar{q}$ and $s\leftrightarrow\bar{s}$ in Eq. (2).

For $E_\nu \ll M_W{}^2/2m \sim 3500$ GeV the W propagator can be set equal to unity. In practice this point-interaction approximation holds for $E_\nu \approx 3500$ GeV (see Fig. 1). We therefore neglect the W propagator and compute

$$\frac{d\sigma_{\nu(\bar{\nu})}}{dy}=\int_0^1\frac{d\sigma_{\nu(\bar{\nu})}}{dx\,dy}dx\ . \quad (3)$$

Using parton-model estimates for the relevant momentum fractions[11] leads to

$$d\sigma_\nu/dE_\mu\cong[0.72+0.06(E_\mu/E_\nu)^2]10^{-38}\text{ cm}^2\text{ GeV}^{-1} \quad (4)$$

and

$$d\sigma_{\bar{\nu}}/dE_\mu\cong[0.69(E_\mu/E_\nu)^2+0.09]10^{-38}\text{ cm}^2\text{GeV}^{-1}\ . \quad (5)$$

Substituting Eqs. (4) and (5) into (1), and assuming a $\nu/\bar{\nu}$ ratio of R, we get

$$S(E_\nu,E_\mu,\theta)=N_A\sigma(R)\frac{dN}{dE_\nu}\left[1+A(R)\left[\frac{E_\mu}{E_\nu}\right]^2\right]\ , \quad (6)$$

where

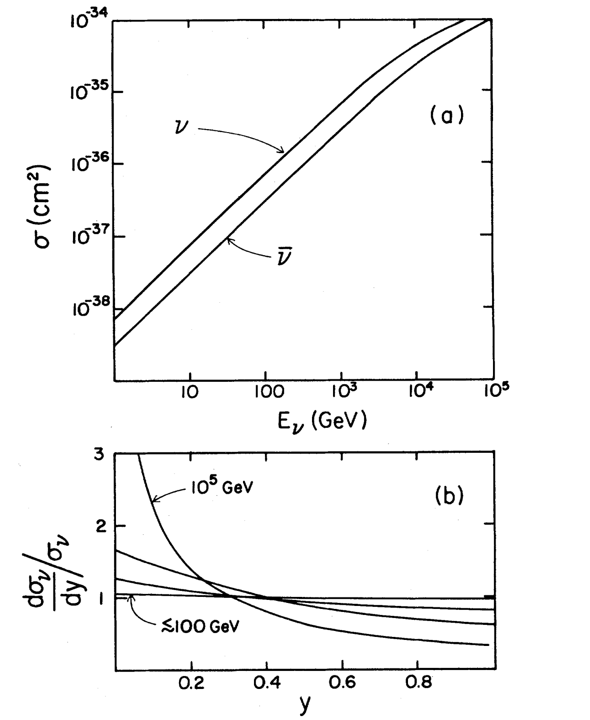

FIG. 1. (a) Cross section for ν ($\bar{\nu}$) on nucleon. (b) Relative cross section vs y for $\nu_\mu+N\rightarrow\mu+X$ for four energies: ≤ 100 GeV, 3000 GeV, 10^4 GeV, and 10^5 GeV.

$$\sigma(R)=\frac{0.72R+0.09}{1+R}\times 10^{-38}\text{ cm}^2\text{ GeV}^{-1}\ ,$$

$$A(R)=\frac{0.69+0.06R}{0.09+0.72R}\ ,$$

and dN/dE_ν is the sum of ν and $\bar{\nu}$ fluxes. At high-neutrino energies ($\gtrsim 3500$ GeV) the charged-current cross section becomes increasingly peaked toward large-muon energies, but the total cross section levels off toward a logarithmic, rather than linear, increase with E_ν. Because of the steep neutrino spectrum, these two changes tend to compensate each other in their effect on the resulting muon spectrum. We find that complete neglect of the W propagator introduces only a 1–2 % error in the calculated muon flux for typical underground detectors.

III. MUON FLUX

The muon flux at an underground detector is the summed effect of the muon luminosity of the surrounding medium taking appropriate account of energy-loss processes between the point of production and the detector. Thus the differential flux of muons at an underground test point is

$$\frac{dN_\mu}{dE_\mu}=\int_{E_\mu}^\infty\left[\int_0^\infty dX\int_{E_\mu}^{E_\nu}dE'_\mu g(X,E_\mu,E'_\mu)\times S(E_\nu,E'_\mu,\theta)\right]dE_\nu\ , \quad (7)$$

where $g(X,E_\mu,E'_\mu)dE_\mu$ is the probability that a muon of initial energy E'_μ has energy between E_μ and $E_\mu+dE_\mu$ after propagating a distance X in rock.

A. Muon propagation

Muon energy-loss processes determine the effective collection area for ν-induced muons through the factor $g(X,E_\mu,E'_\mu)$ in Eq. (2). The energy-loss equation is of the form

$$dE/dX=-\alpha-\beta E \tag{8}$$

with

$$\alpha\cong 2\ \mathrm{MeV/(g/cm^2)}$$

and

$$\beta\cong 3.9\times 10^{-6}\ (\mathrm{g/cm^2})^{-1}$$

for muon energies in the GeV-TeV range.[12] The first term in Eq. (8) is due to ionization energy loss and the last term to bremsstrahlung and photonuclear interactions. The average range-energy relation is thus

$$E_\mu=F(X)\equiv(E'_\mu+\alpha/\beta)e^{-\beta X}-\alpha/\beta\ . \tag{9}$$

We have computed $g(X,E_\mu,E'_\mu)$ with a full Monte Carlo treatment of muon propagation in rock taking account of the correct energy dependence of the various energy-loss processes. We compare below the result of this detailed numerical procedure with an approximate, analytic treatment which uses the average values stated above for α and β. The approximate analytic result is sufficiently accurate (see below) and simple so that it is worthwhile to display it.

B. Analytic approximation

The approximation consists of using the expression

$$g(X,E_\mu,E'_\mu)=\delta(E_\mu-F(X))=\frac{\delta(X-X_0)}{\alpha(1+\beta E_\mu/\alpha)}\ , \tag{10}$$

where

$$\beta X_0=\ln\frac{E'_\mu+\alpha/\beta}{E_\mu+\alpha/\beta}\ .$$

Then the expression inside the square brackets in Eq. (7) is

$$\frac{dN_\mu}{dE_\mu dE_\nu}=\frac{N_A\sigma(R)}{\alpha}\frac{dN}{dE_\nu}\times\frac{1}{1+E_\mu/\epsilon}\left[E_\nu-E_\mu+\frac{A(R)}{3}\frac{E_\nu{}^3-E_\mu{}^3}{E_\nu{}^2}\right], \tag{11}$$

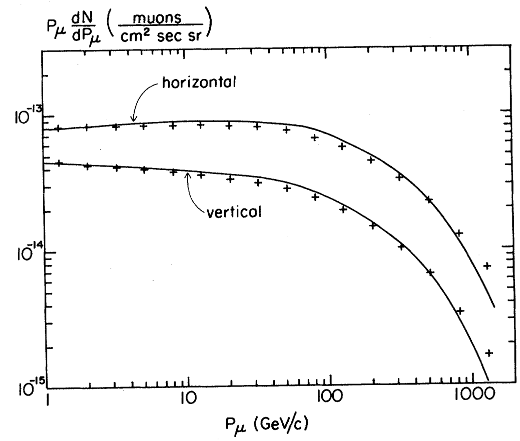

FIG. 2. Comparison of Monte Carlo (+) with analytic result obtained by integrating Eq. (11) over all E_ν.

where $\alpha/\beta\equiv\epsilon=510$ GeV.

C. Muon energy spectrum

The muon energy spectrum is obtained by integrating Eq. (11) over E_ν. In Fig. 2 we show a comparison between the spectrum obtained in this way with that obtained from the full Monte Carlo calculation of muon propagation. The effect of neglecting range straggling in the analytic approximation only becomes important at the highest muon momenta where the neutrino spectrum is steep. It is clear that the analytic approximation is good to within 10% or better.

IV. MUON RESPONSE

The response function is the distribution of neutrino energies that gives rise to a certain group of muons, for example those with energies between $E_{\min}$ and $E_{\max}$. In typical experiments, the muon energy is not measured, but one can distinguish stopping from through-going muons. For numerical examples we take $1\le E_\mu\le 4$ GeV as a definition of stopping muons (range between $\sim$4 and 20 m of water). Results for other values follow directly from the analytic expression, which we use because of its simplicity and because it gives an adequate quantitative approximation.

For both stopping and through-going muons one needs the integral

$$\frac{dN_\mu}{dE_\nu}=\int_{E_{\min}}^{E_{\max}}\frac{dN_\mu}{dE_\mu dE_\nu}dE_\mu$$
$$=\frac{N_A\sigma(R)}{\alpha}\frac{dN}{dE_\nu}\frac{\epsilon^4}{3E_\nu{}^2}\left[A_1\ln\frac{D_{\max}}{D_{\min}}+A_2(D_{\max}-D_{\min})+A_3(D_{\max}{}^2-D_{\min}{}^2)+A_4(D_{\max}{}^3-D_{\min}{}^3)\right]. \tag{12}$$

Here $D \equiv 1+E/\epsilon$ and

$$A_1\epsilon^3 = 3E_\nu{}^3 + 3\epsilon E_\nu{}^2 + A(R)E_\nu{}^3 + A(R)\epsilon^3,\quad \epsilon^3 A_2 = -3[E_\nu{}^2\epsilon + A(R)\epsilon^3],\quad A_3 = \tfrac{3}{2}A(R),\quad A_4 = -A(R)/3\,.$$

For $E_\nu \ll \epsilon, D_\mu \sim 1$ in Eq. (12) and the expression simplifies to

$$\frac{dN_\mu}{dE_\nu} = \frac{N_A\sigma(R)}{\alpha}\frac{dN}{dE_\nu}(E_{\max}-E_{\min}) \times \left[\left[1+\frac{A(R)}{3} \right] E_\nu - \frac{E_{\max}+E_{\min}}{2} - \frac{A(R)}{12}\frac{(E_{\max}{}^3+E_{\max}{}^2E_{\min}+E_{\max}E_{\min}{}^2+E_{\max}{}^3)}{E_\nu{}^2} \right]. \tag{13}$$

For through-going muons, for which $E_{\max}=E_\nu$, the leading term in Eq. (13) is

$$\sim 9.1\times 10^{-13}\frac{dN}{dE_\nu}[E_\nu\ (\mathrm{GeV})]^2 \quad \text{for } R=1.2.$$

One power of E_ν comes from the linear increase in muon range with energy when only ionization loss is important; the other power comes from the linear increase of σ_ν for $2mE_\nu \ll M_W$. At high energies both factors cut off, the former when bremsstrahlung becomes an important energy-loss mechanism ($E_\nu \gtrsim 510$ GeV) and the latter when the W propagator becomes important ($E_\nu \gtrsim 3500$ GeV).

In Fig. 3 we show the logarithmic response $E_\nu dN/dE_\nu$ plotted vs $\log E_\nu$ averaged over all directions from below the horizontal. The shape of the response curve depends only weakly on zenith angle. Equal areas on such a semilogarithmic plot correspond to equal contributions to the muon flux.

For stopping muons defined as above the median neutrino energy is about 5 GeV, with only about 5% of the stopping muons originating from neutrinos with $E_\nu > 50$ GeV. For through-going muons the median energy is around 100 GeV (somewhat lower for vertical and somewhat higher for nearly horizontal muons), with about 10% coming from $E_\nu > 1000$ GeV.

In Fig. 4 we show the angular distribution of the muon flux. Integrating over 2π (upward) solid angle gives 4.8×10^{-13} upward stopping muons/(cm^{2}sec) and 13.8×10^{-13} upward through-going muons/(cm^{2}sec). For 400-m^2 area as in the Irvine-Michigan-Brookhaven (IMB) experiment, this corresponds to 0.17 upward stopping muons and 0.48 upward through-going muons per day. Fluxes for other definitions of stopping and through-going are shown in Table I. The columns labeled $R\uparrow$ in Table I have been obtained with the assumption that $R=1.2+0.69\ln(E_\nu)$, which represents the increase with energy expected because of the increasing importance of neutrinos from kaon decay.[1] Results are not very sensitive to the assumption about R.

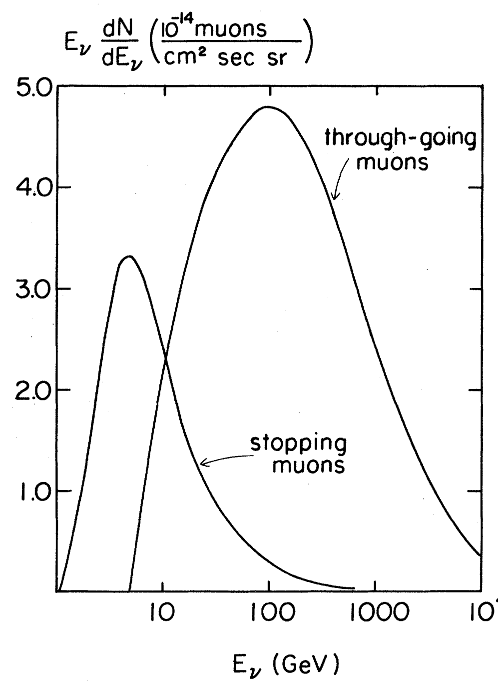

FIG. 3. Distribution of primary energies that give rise to stopping muons with $1 \le E_\mu \le 4$ GeV and to muons with $E_\mu > 4$ GeV assuming $R=1.2$ and averaging over all arrival directions from below the horizontal.

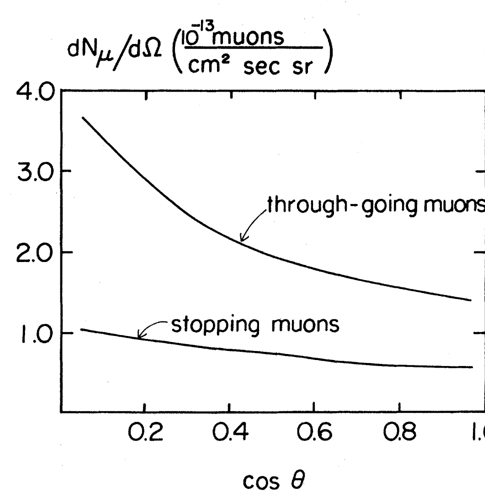

FIG. 4. Stopping muons ($1 \le E_\mu \le 4$ GeV) and through-going muons ($E_\mu \ge 4$ GeV) as a function of zenith angle. Here $\cos\theta=1$ is vertically upward and $\cos\theta=0$ is horizontal. $R=1.2$ is assumed.

TABLE I. Muon rates (in 10^{-13} cm^{-2}sec^{-1}) for upward (0°–60°) and horizontal-upward (60°–90°) muons. $R=\nu/\bar{\nu}$ and $R\uparrow$ has R increasing with energy (see text).

$E_{\min}$ (GeV)		Stopping (≤ 2 GeV) $R=1.2$	$R\uparrow$	Stopping (≤ 4 GeV) $R=1.2$	$R\uparrow$	Through-going $R=1.2$	$R\uparrow$
0.2							
	0–60°	4.17	4.24	5.59	5.70	14.2	14.8
	60–90°	3.16	3.21	4.15	4.23	9.26	9.6
	Total	7.32	7.45	9.74	9.93	23.5	24.4
0.5							
	0–60°	2.72	2.78	4.10	4.20	12.8	13.3
	60–90°	2.03	2.07	2.99	3.06	8.1	8.45
	Total	4.74	4.85	7.09	7.27	20.9	21.8
1.0							
	0–60°	1.40	1.43	2.79	2.87	11.4	12.0
	60–90°	1.02	1.04	1.99	2.04	7.1	7.42
	Total	2.42	2.47	4.78	4.91	18.5	19.4
2.0							
	0–60°			1.40	1.44	10.1	10.6
	60–90°			0.98	1.01	6.1	6.39
	Total			2.37	2.45	16.2	17.0
4.0							
	0–60°					8.65	9.11
	60–90°					5.12	5.38
	Total					13.8	14.5
7.0							
	0–60°					7.52	7.93
	60–90°					4.36	4.59
	Total					11.9	12.5
10.0							
	0–60°					6.81	7.19
	60–90°					3.89	4.10
	Total					10.7	11.30

The deviation between the ν ($\bar{\nu}$) direction and that of the observed muon will somewhat flatten the angular distribution in Fig. 4. For incident neutrinos, the median deviation is approximately[13] $\Delta\theta \sim (1/\pi E_\nu)^{1/2}$ for $E_\nu > 10$ GeV. Using the median $\Delta\theta$ at the median energy for through-going muons, we estimate the magnitude of the change in $dN_\mu/d\Omega$ in Fig. 4 to be less than 5% from this source.

V. DISCUSSION

It is interesting to compare results of these calculations with various experimental results. For the average flux of upward ($180° > \theta > 130°$) muons above 2 GeV we find 1.9×10^{-13} muons/cm^{2}sec sr, consistent with the measured value[3] $1.92\pm 0.44\times 10^{-13}$. For the horizontal flux of all muons we find 6.2×10^{-13}/cm^{2}sec sr somewhat higher than the measured value[1] $(4.59\pm 0.42)\times 10^{-13}$/cm^{2}sec sr. We also find that the angular dependence of the rate of muons of all energy is very similar to the results (both measured and calculated) of Ref. 2. A recent report[14] of the flux of upward muons averaged over all angles 0–90° gives 0.50 ± 0.07/day in 500 m^2 with a detection efficiency estimated at 0.7. From the table the corresponding calculated number is 0.51. Thus, with the possible exception of Ref. 1, the measurements are completely consistent with conventional expectation.

From the point of view of searching for neutrino oscillations, the most important point is the large contribution to the observed flux of upward muons from high-energy neutrinos which are least sensitive to possible oscillation phenomena. The median energy of the ν_μ parents of upward muons with $E_\mu > 2$ GeV is about 100 GeV. The corresponding number for contained neutrino interactions is of order 1 GeV. The sensitivity to Δm^2 is thus significantly greater with contained neutrino interactions than with upward muons.

Geophysical ν-oscillation searches with upward and horizontal muons to date involve comparison between a measured and a calculated rate. With a sufficiently deep detector capable of determining the muon direction to within a few degrees it will also be feasible to make a direct comparison between muons from below the horizon with muons from above the horizon. In principle one wants to compare muons with a zenith angle $\theta < 90°$ with the flux of muons at $\theta' = 180 - \theta$. Because of the geometrical symmetry, a difference in counting rate between θ and $180° - \theta$ would signal neutrino-flavor oscillations independent of any calculation.[15] (Interpretation of the effect would still depend on folding an oscillation model with the calculated spectrum of parent neutrinos.) In practice, to obtain sufficient statistics, one would compare the flux for two conical wedges, say, $60° < \theta < 85°$ and $95° < \theta < 120°$. From Fig. 4 we can see that each of these regions would give a counting rate equal to about one half the total counting rate from below the horizon.

To determine the sensitivity of a particular detector for neutrino-oscillation searches in general is difficult. It is necessary to fold the decay-length distribution (which depends on angular resolution) and the energy distribution with the oscillation probability $P(\nu_\mu \rightarrow \nu_\mu)$ for each oscillation model taking account of effects of propagation in matter.[16]

Dass and Sarma[17] have given an analytical treatment of the effect of path-length distributions in the presence of matter oscillations at neutrino energies of several GeV. Stenger[18] has used a Monte Carlo approach to assess the sensitivity of DUMAND (deep underwater muon and neutrino detector) to neutrino oscillations in the TeV range. In either approach, the distribution of energies of parents of observed muons, as calculated here, is relevant. It could be used in conjunction with the analysis of Dass and Sarma to give a complete evaluation of effects of neutrino oscillations on upward muons. A hybrid approach might be simpler. One could use appropriate distributions of the type shown in Fig. 3 to select energies of neutrino parents of upward muons in each angular bin and then obtain the corresponding path length and oscillation probability. This would avoid full Monte Carlo treatment of neutrino interactions and muon propagation.[19]

ACKNOWLEDGMENTS

We thank Don Reeder, Francis Halzen, and David Cline for hospitality at the University of Wisconsin where this work was initiated. This work was supported in part by the U.S. Department of Energy under Contract No. DE-AC02-78ER05007 and by the National Science Foundation.

---

*On leave from Institute for Nuclear Reserach and Nuclear Energy, Sofia, Bulgaria.

[1] M. F. Crouch *et al.*, Phys. Rev. D **18**, 2239 (1978).

[2] M. R. Krishnaswamy *et al.*, Pramana **19**, 525 (1982).

[3] M. M. Boliev *et al.*, in *17th International Cosmic Ray Conference, Paris, 1981, Conference Papers* (Centre d'Études Nucleaires, Saclay, 1981), Vol. 7, p.106.

[4] For reviews of neutrino oscillations see, e.g., A. K. Mann and H. Primakoff, Phys. Rev. D **15**, 655 (1977); S. M. Bilenky and B. Pontecorvo, Phys. Rep. **41**, 225 (1978).

[5] R. E. Lanou, Jr., in *Proceedings of the 1982 DPF Summer Study on Elementary Particle Physics and Future Facilities, Snowmass, Colorado,* edited by R. Donaldson, R. Gustafson, and F. Paige (Fermilab, Batavia, Illinois, 1982), p. 538.

[6] D. S. Ayres *et al.*, Phys. Rev. D **29**, 902 (1984).

[7] R. Cowsik, Yash Pal, and S. N. Tandon, Proc. Indian Acad. Sci. **53**, 217 (1966), and earlier references.

[8] T. K. Gaisser, Todor Stanev, S. Bludman, and H. Lee, Phys. Rev. Lett. **51**, 223 (1983); in *Proceedings of the Fourth Workshop on Grand Unification, University of Pennsylvania, 1983,* edited by H. A. Weldon, P. Langacker, and P. J. Steinhardt (Birkhäuser, Boston, 1983), p. 87.

[9] L. V. Volkova, Yad. Fiz. **31**, 784 (1980) [Sov. J. Nucl. Phys. **31**, 1510 (1980)]; in *Proceedings of the 1978 DUMAND Summer Workshop, LaJolla, California,* edited by A. Roberts (Scripps Institute of Oceanography, LaJolla, 1979), Vol. 1, p. 75.

[10] L. B. Okun, *Leptons and Quarks* (North-Holland, Amsterdam, 1982), p. 149.

[11] R. Field and R. P. Feynman, Phys. Rev. D **15**, 2590 (1977).

[12] Todor Stanev, Bartol Technical Report No. BA-83-41, 1983 (unpublished).

[13] T. K. Gaisser, in Proceedings of the Fourth Moriond Astrophysics Meeting, LaPlagne, France, 1984, Bartol Report No. BA-84-21 (unpublished).

[14] R. M. Bionta *et al.*, reported at the ICOBAN 84 meeting, Park City, Utah, 1984 (unpublished); J. C. Vander Velde (private communication).

[15] The situation here is unlike that for contained interactions, where, because of the lower energies involved, the geometrical symmetry is upset by geometrical effects. [T. K. Gaisser, in *Science Underground,* proceedings of the Workshop, Los Alamos, 1982, edited by M. M. Nieto *et al.* (AIP, New York, 1983), p. 203. See also Refs. 6 and 8.]

[16] L. Wolfenstein, Phys. Rev. D **17**, 2369 (1978); V. Barger, *et al., ibid.* **22**, 2718 (1980).

[17] G. V. Dass and K. V. L. Sarma, Phys. Rev. D **30**, 80 (1984).

[18] V. J. Stenger, in *Proceedings of the 1980 DUMAND Symposium, Honolulu,* edited by V. J. Stenger (Hawaii DUMAND Center, Honolulu, 1981), Vol. 2, p. 37. This calculation does not include effects of propagation in matter.

[19] The muon threshold in DUMAND is about 100 GeV so the calculation of parent energy distribution in that case requires inclusion of the W propagator in Eq. (4) with a 100-GeV threshold, the median ν energy for ν_μ-induced muons is more than an order of magnitude higher for DUMAND than for the underground detectors. Thus the sensitivity to the Δm^2 oscillation parameter is correspondingly less.